

Reduced Size Frequency Agile Microwave Circuits Using Ferroelectric Thin-Film Varactors

Errikos Lourandakis, *Member, IEEE*, Matthias Schmidt, *Member, IEEE*, Stefan Seitz, *Member, IEEE*, and Robert Weigel, *Fellow, IEEE*

Abstract—A new concept for tunable and reduced size microwave circuits is presented based on barium–strontium–titanate (BST) varactors. The proposed design methodology relies on substitution of quarter-wavelength transmission line segments with their equivalent low-pass structures. The ferroelectric BST-varactors are used as tuning elements and allow for a frequency agile behavior and size reduction of the circuit. Candidates for this methodology are quarter-wavelength based circuits such as Wilkinson power dividers and branch-line couplers. Prototype boards for both topologies were implemented and characterized through scattering parameter measurements. For the implemented Wilkinson divider a tuning range from 1.7 to 2.1 GHz is achieved. The insertion loss in both output paths varies from 0.6 to 1.2 dB while maintaining a worst case amplitude- and phase difference of 0.5 dB and 9° , respectively, for all operating cases. The isolation between the two output ports exceeded 25 dB over the whole tuning range. The implemented branch-line coupler exhibits a tuning range from 1.8 to 2.3 GHz with a maximum insertion loss of 2.7 dB while maintaining worst case amplitude- and phase difference of 0.4 dB and $90^\circ \pm 5^\circ$, respectively. Port matching and isolation levels of more than 15 dB are exhibited at all bias conditions.

Index Terms—Couplers, ferroelectric capacitors, power dividers, tunable circuits and devices.

I. INTRODUCTION

THE continuously rising number of communication standards, which have to be covered by modern mobile radios, calls for reconfigurable and frequency agile front-end components. Already known techniques of designing microwave systems can be adapted in order to incorporate new functionalities, e.g., tunability and thus enable new system architectures with reduced number of functional blocks. Ferroelectric materials have been used extensively for tuning purposes. Among the possible ferroelectric materials for such applications, barium–strontium–titanate (BST) is probably the most suitable candidate due to its relative high permittivity and well known electrical performance. Tunable passive components based on BST, like ferroelectric varactors, have introduced a whole new group of tunable

subsystems, e.g., filters [1], [2], phase shifters [3], [4], matching networks [5], [6], switches [7], [8], and baluns [9]. Furthermore, active microwave circuits such as tunable voltage controlled oscillators [10], [11] and dynamically tunable power amplifiers [12], [13] have been reported. Previously we presented a reduced size and tunable power divider [14] based on BST-varactors. In this paper this new technique is generalized and applied to both, the Wilkinson divider [15] and the hybrid branch-line coupler. Additionally to frequency agility, as reported also in [16], [17], our approach leads to size reduction. The operating principle is discussed in Section III and is enhanced with a new functionality by introducing the ferroelectric varactors. For the first time, a successful implementation for transmission line based circuits is demonstrated.

The familiar narrowband performance of $\lambda/4$ based topologies is obtained for different operating frequencies. This tuning functionality enables a frequency agile operation. At the same time, size reduction is achieved which is a step forward to higher integration levels in future front-end architectures. Designing high performance circuits based on tunable components is a challenging task and is mainly influenced by the structure of the component, the electrical behavior, and also its assembly within the circuit. Therefore all of these aspects are discussed in Sections II–V. In Section II, the used ferroelectric varactors and their electrical performance is presented, while in Section III the technique of substitution of the $\lambda/4$ segments with their equivalent low-pass structures is discussed. In Section IV, this technique is applied for the Wilkinson power divider and the hybrid branch-line coupler. Finally, in Section V, the BST-varactor based implemented tunable and reduced size prototype circuits and the corresponding measurement results are shown.

II. FERROELECTRIC THIN-FILM VARACTORS

BST is a composite material, consisting of barium–titanate and strontium–titanate forming a mixed crystal, represented as $\text{Ba}_x\text{Sr}_{(1-x)}\text{TiO}_3$ where the doping ratio x determines the phase transition point between ferroelectric and paraelectric phase. So far, the potential usage of BST in microwave circuits has been investigated mostly by academic research groups. Over the last years noticeable effort has been done also from industrial site in order to establish this technology for commercial high volume applications [18], [19].

Ferroelectric BST-varactors can be processed either as a metal–insulator–metal (MIM) parallel plate structure, as indicated in Fig. 1, or as planar interdigital capacitors (IDC) [20], [21]. For the parallel plate capacitor the ferroelectric film of height d is located between the two metal electrodes. In this case, platinum (Pt) is the electrode metal which is covered

Manuscript received April 23, 2008; revised July 17, 2008. First published November 07, 2008; current version published December 05, 2008. This work was supported under MARIO Project FKZ 01BU570, which is funded and supported by the Federal Ministry of Education and Research (BMBF), Germany.

E. Lourandakis and R. Weigel are with the Institute for Electronics Engineering, University of Erlangen–Nuremberg, D-91058 Erlangen, Germany (e-mail: lourandakis@lfe.de; weigel@lfe.de).

M. Schmidt and S. Seitz are with the Research and Development New Products Department, EPCOS AG, D-81671 Munich, Germany.

Color versions of one or more of the figures in this paper are available online at <http://ieeexplore.ieee.org>.

Digital Object Identifier 10.1109/TMTT.2008.2006807

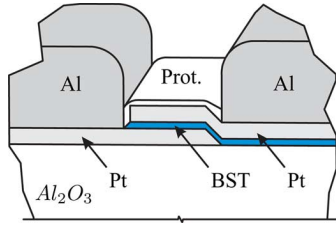


Fig. 1. Typical structure of ferroelectric thin-film MIM-varactor.

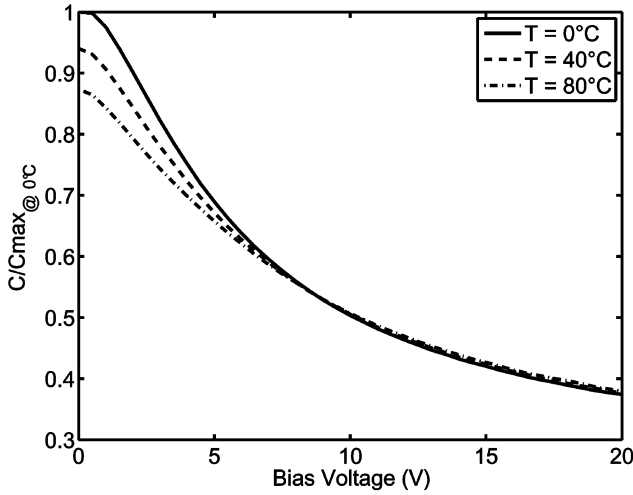


Fig. 2. On-wafer measured capacitance of a 5 pF varactor for different temperature conditions. Data from [14].

by an additional aluminum (Al) layer. The active area of the parallel plate capacitor is furthermore covered with a protecting isolating layer. The whole material stack is based on a ceramic alumina (Al_2O_3) substrate. Different electrode materials and layer configurations have been reported as well [22], [23]. An electrical field \vec{E} is built by applying a bias voltage V on the electrodes. This field, which is straightforward related to the bias voltage as V/d , alters the permittivity of the BST-film and can be described in a mathematical manner [24].

The voltage dependence of the BST-varactors is shown in Fig. 2 for a capacitor of 5 pF nominal capacitance. The measurements were taken with an Agilent E4991A RF-impedance analyzer for frequencies up to 3 GHz by an on-wafer procedure and after the appropriate short open load (SOL) calibration. The capacitance value C as well as the varactor quality factor Q were extracted from the measured input admittance Y according to (1) and (2), respectively, as follows, where in the frequency region of interest the measured quality factor values were around 40:

$$C = \frac{\Im\{Y\}}{2\pi f} \quad (1)$$

$$Q = \frac{\Im\{Y\}}{\Re\{Y\}}. \quad (2)$$

The maximum capacitance is always obtained at zero bias. For higher temperatures the relative permittivity ϵ_r is decreasing, as predicted by the Ginzburg–Landau theory [25], since the temperature in the crystal moves far away from the

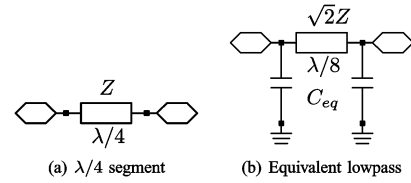


Fig. 3. Quarter-wavelength transmission line segment and its equivalent low-pass structure.

phase transition point. Therefore the obtained capacitance is reduced since $C = \epsilon_r \epsilon_0 A/d$ where A is the effective electrode area. At low temperatures a tunability, defined as $(\epsilon_{r\max} - \epsilon_{r\min})/\epsilon_{r\max}$, of more than 60% is achievable at a bias voltage of 20 V. An additional phenomenon that takes place when a bias voltage is applied are the induced acoustic resonances. The perovskite-type BST crystal is symmetric in absence of an electrical field. By applying a bias voltage the crystal becomes asymmetric, thus piezoelectric, and introduces a parasitic resonance to the layered structure [26], [27]. The overall electrical behavior of BST thin-film varactors can be described by equivalent models [28], thus allowing accurate linear and nonlinear simulations during the circuit design procedure.

III. EQUIVALENT QUARTER-WAVELENGTH SEGMENTS

The proposed methodology is based on the principle of substituting $\lambda/4$ transmission line segments of initial characteristic impedance Z with equivalent low-pass structures [29]. The resulting new transmission line segments can be made significantly shorter by raising their characteristic impedance level to $\sqrt{2}Z$ and add shunt capacitors at the ends, as depicted in Fig. 3.

The capacitance value for the equivalent low-pass structure can be calculated by comparing the network parameter matrix of the quarter-wavelength segment with the corresponding matrix of the low-pass structure. For the general transmission line segment of characteristic impedance Z and electrical length θ , the $ABCD$ matrix is given as

$$M = \begin{bmatrix} A & B \\ C & D \end{bmatrix} = \begin{bmatrix} \cos \theta & jZ \sin \theta \\ \frac{j \sin \theta}{Z} & \cos \theta \end{bmatrix}. \quad (3)$$

For the case where $\theta = \pi/2$, the matrix is reduced to

$$M = \begin{bmatrix} 0 & jZ \\ \frac{j}{Z} & 0 \end{bmatrix}. \quad (4)$$

The overall $ABCD$ matrix of the equivalent low-pass structure can be calculated by multiplying the individual chain matrices of the two shunt capacitors and the reduced length transmission line segment. Thus, $M_{\text{total}} = M_1 \cdot M_2 \cdot M_3$, where

$$M_1 = M_3 = \begin{bmatrix} A & B \\ C & D \end{bmatrix} = \begin{bmatrix} 1 & 0 \\ j\omega C_{\text{eq}} & 1 \end{bmatrix} \quad (5)$$

$$M_2 = \begin{bmatrix} A & B \\ C & D \end{bmatrix} = \begin{bmatrix} \frac{\sqrt{2}}{2} & jZ \\ \frac{j}{2Z} & \frac{\sqrt{2}}{2} \end{bmatrix}. \quad (6)$$

The resulting overall $ABCD$ matrix M_{total} is then given as

$$\begin{bmatrix} \frac{-\omega C_{\text{eq}} Z \sqrt{2} + 1}{\sqrt{2}} & jZ \\ j \left(\frac{2\sqrt{2}\omega C_{\text{eq}} Z + 1 - 2\omega^2 C_{\text{eq}}^2 Z^2}{2Z} \right) & \frac{-\omega C_{\text{eq}} Z \sqrt{2} + 1}{\sqrt{2}} \end{bmatrix}. \quad (7)$$

Comparing (4) and (7) results in a single solution for C_{eq}

$$C_{\text{eq}} = \frac{1}{\omega\sqrt{2}Z} = \frac{1}{2\pi f\sqrt{2}Z}. \quad (8)$$

By presenting a closed formula in (8) it is possible to design fully scalable equivalent quarter-wavelength transmission line segments. For each starting impedance Z and resonance frequency f a single capacitance value C_{eq} is calculated. On the other hand, it is evident that by changing the capacitance value C_{eq} the resonance frequency f is altered. Limiting factors could be only the resulting impedance values for real implementations, e.g., in microstrip technology and the varying line impedance for different frequencies. Nevertheless, by using tunable capacitors, such as BST-varactors, a tuning functionality is achieved. Understanding this operational principle yields to designs of more complex topologies which are based on $\lambda/4$ segments.

IV. REDUCED SIZE MICROWAVE CIRCUITS

A. Wilkinson Divider

The power divider proposed by Wilkinson is based on quarter-wavelength transmission line segments and is presented in Fig. 4(a). The input and output port impedances are Z_0 while the $\lambda/4$ segments have a characteristic impedance of $\sqrt{2}Z_0$. The output branches are connected through a resistor with $R = 2Z_0$, thus enabling impedance matching at all ports and isolation between them at the $\lambda/4$ resonance frequency. Symmetric power splitting is achieved with no phase difference, $\Delta\phi = 0$, for the two transmission paths. The reduced size topology is presented in Fig. 4(b). The new transmission line segments have a shorter electrical length and a higher characteristic impedance. Lumped capacitors are used in order to compensate for the shorter propagation path. The $\lambda/4$ transmission line segment of impedance $\sqrt{2}Z_0$ can be substituted by an equivalent segment of length $\lambda/8$ with an impedance of $2Z_0$ by adding two lumped capacitors to the transmission line with a capacitance value of

$$C_{\text{eq}} = \frac{1}{4\pi f Z_0}. \quad (9)$$

B. Branch-Line Coupler

The branch-line coupler consists also of $\lambda/4$ transmission line segments which form a four-port network. The inserted power at port 1 is equally divided at the output ports 2 and 3 at the $\lambda/4$ resonance frequency. At this point port 4 is isolated as well. The output signals have a phase difference of $\Delta\phi = 90^\circ$.

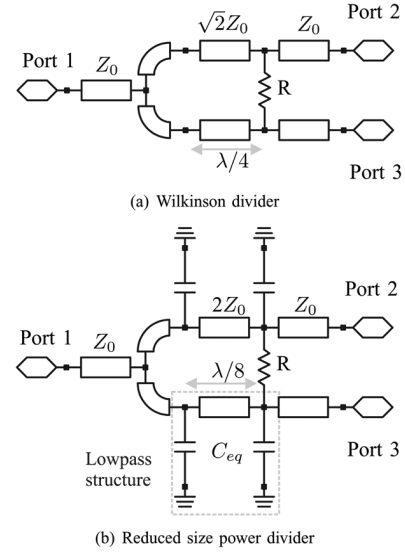


Fig. 4. Power divider topologies.

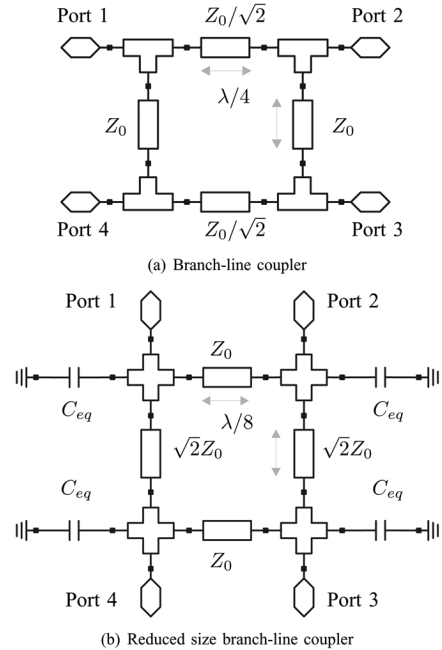


Fig. 5. Branch-line coupler topologies.

The characteristic impedance of the series branches is $Z_0/\sqrt{2}$, whereas the parallel branches have a characteristic impedance of Z_0 , as presented in Fig. 5(a).

The reduced size topology in Fig. 5(b) uses the same principle as before. The series $\lambda/4$ branches with $Z_0/\sqrt{2}$ are substituted by low-pass segments with Z_0 and shunt capacitors $C_1 = 1/(2\pi f Z_0)$. The parallel $\lambda/4$ segments with Z_0 are substituted by low-pass segments with $\sqrt{2}Z_0$ and shunt capacitors $C_2 = 1/(2\pi f \sqrt{2}Z_0)$. In order to reduce the overall complexity the shunt capacitors at the transmission line ends were combined into the value

$$C_{\text{eq}} = C_1 + C_2 = \frac{1 + \sqrt{2}}{2\pi f \sqrt{2}Z_0}. \quad (10)$$

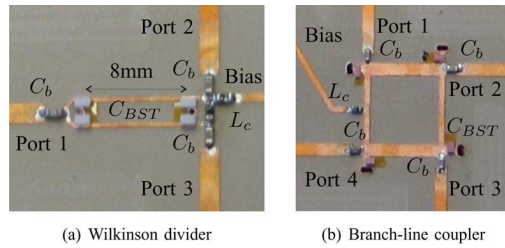


Fig. 6. Fabricated prototype boards.

This equivalent capacitance serves as a shunt element for both transmission line segments that meet at each port, thus allowing for a more compact design with reduced complexity.

V. PROTOTYPE IMPLEMENTATION AND RESULTS

Both previously discussed reduced size topologies use fixed capacitors in order to achieve the targeted narrowband performance at the circuit resonance frequency. As mentioned before, there is a possibility of introducing a tuning functionality by changing the capacitor value C_{eq} . Ferroelectric BST-varactors can serve as such tuning elements. Prototype boards of the proposed tunable microwave circuits were implemented on a Rogers RO3010 substrate with height $h = 1.27$ mm and dielectric constant $\epsilon_r = 10.2$.

The circuit traces of the fabricated prototypes are depicted in Fig. 6. Additional biasing components such as dc-block capacitors C_b , at all RF-ports, and RF-choke inductors L_c are used in order to establish the proper biasing conditions for the BST-varactors. The dc-block capacitors behave at these frequencies nearly as a through connection while the choke inductors present a high impedance path to the RF signal traveling on the microstrip lines. Therefore, the impact of the biasing elements can be almost neglected. It is worth mentioning that by using the proposed design it is possible to tune simultaneously all varactors. The bias circuitry is simplified since a single tuning voltage is needed.

All BST-varactors were assembled in a flip-chip procedure in order to eliminate the resulting parasitic wire inductance and the associated loss mechanisms of conventional ball-wedge or wedge-wedge assemblies. These interconnection parasitics are especially troublesome for higher operating frequencies and broadband applications since the feeding wire inductance causes a rapidly rising effective capacitance. Furthermore flip-chip interconnections lead to smaller footprints compared to wire assemblies since there is no need for large gaps between the metal traces. Gold stud bumps were placed on the varactor chip pads and connected to the metal traces of the board via a conductive adhesive. The prototypes were characterized through S -parameter measurements which were taken with a Rohde & Schwarz ZVB8 vector network analyzer.

A. Wilkinson Divider

The measured transmission and reflection parameters of the tunable and reduced size power divider are presented for three discrete bias states in Figs. 7–9. From (9), the varactor values for the targeted frequency region are calculated. For

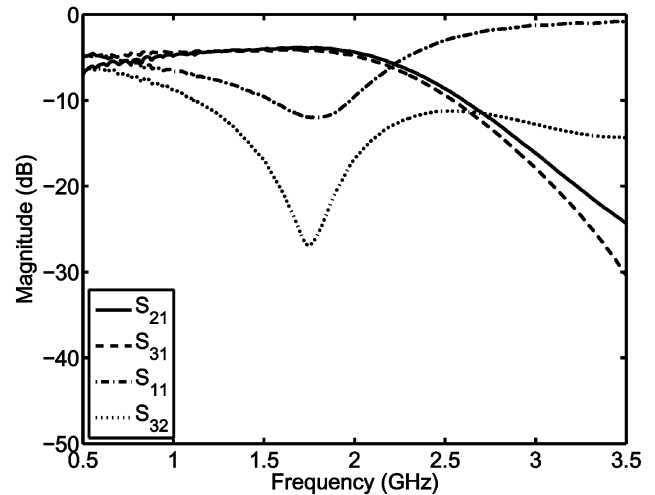


Fig. 7. Measured transmission and reflection S -parameters for tunable Wilkinson divider prototype at bias state $U_{\text{bias}} = 2$ V. Data from [14].

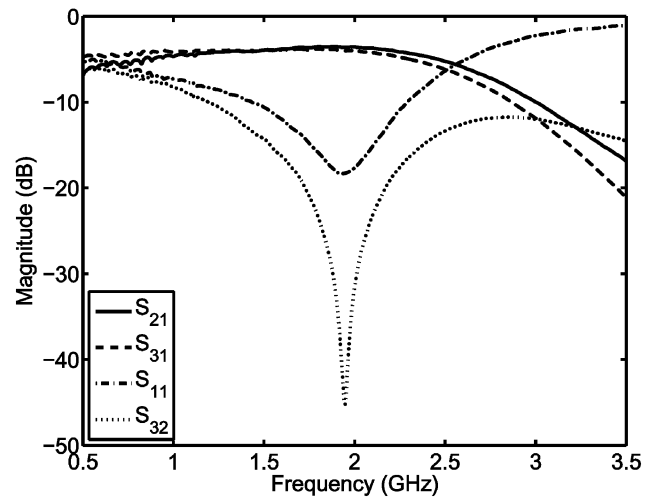


Fig. 8. Measured transmission and reflection S -parameters for tunable Wilkinson divider prototype at bias state $U_{\text{bias}} = 6$ V. Data from [14].

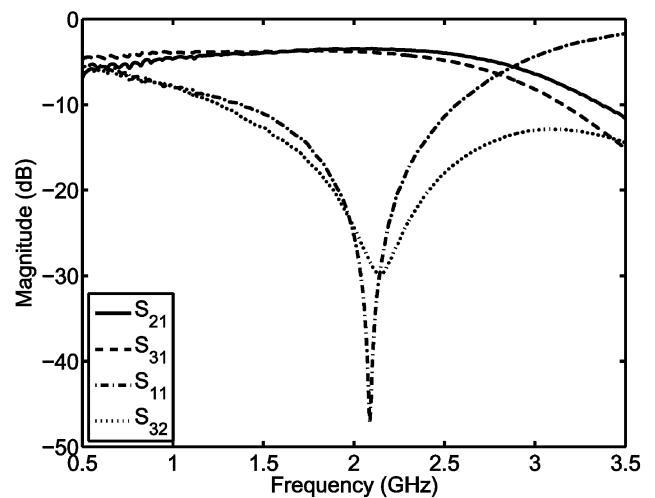


Fig. 9. Measured transmission and reflection S -parameters for tunable Wilkinson divider prototype at bias state $U_{\text{bias}} = 17$ V. Data from [14].

the implemented prototype varactors with nominal capacitance $C_{eq} = 1$ pF serve as tuning elements. As demonstrated

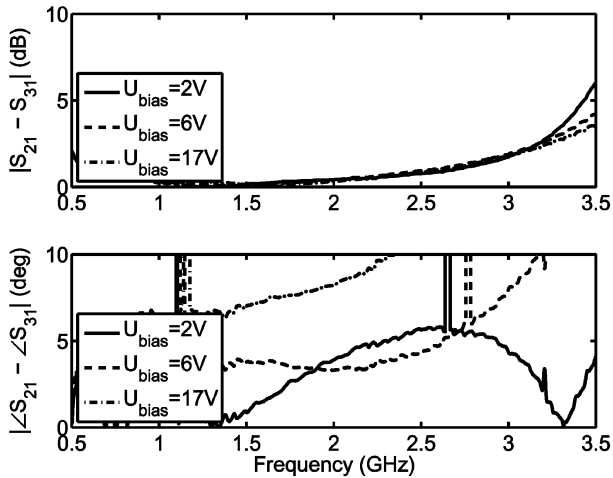


Fig. 10. Measured amplitude (*top*) and phase difference (*bottom*) for the transmission paths of the power divider.

in [14] excellent agreement between simulation and measurements is obtained by using the equivalent varactor models from [28].

As can be seen the well known narrowband performance of the original Wilkinson divider is obtained for different frequencies. Tuning the varactor value leads to different resonance frequencies for the equivalent $\lambda/4$ transmission line segments. A continuous tuning range from 1.7 to 2.1 GHz is obtained. The insertion loss of the circuit, compared to the ideal 3 dB power splitting, varies from 0.6 to 1.2 dB within the operating bandwidth of each state. The resulting amplitude and phase difference for the two transmission paths is depicted in Fig. 10. Symmetrical power splitting is achieved, in both amplitude and phase, thus fulfilling the divider operation. The indicated small differences are mainly due to varactor value tolerances. The worst case amplitude- and phase difference is 0.5 dB and 9° , respectively.

The advantage provided by the tuning functionality concerns mainly the isolation between the output ports. The input return loss of the implemented prototype does not behave the same way due to possible varactor tolerances and some detuning of the transmission lines. In this frequency region there are several communication bands allocated, thus frequency selectivity is desired. As discussed in [14], compared to a reduced size power divider with fixed capacitors improved isolation is achieved at the other operating bias states. All figures reveal the inherent low-pass behavior, thus harmonic radiation would be suppressed significantly when considering an operation in a transceiver front-end system.

B. Branch-Line Coupler

For the branch-line coupler varactors with nominal capacitance $C_{\text{eq}} = 3$ pF serve as tuning elements, according to (10). Similar to the Wilkinson divider prototype, excellent agreement between simulation and measurements is obtained, as indicated in Fig. 11. All designs and simulations were carried out with Agilent's ADS 2008 and Momentum tools. Minor deviations are caused by varactor value tolerances and mismatches. The S -parameter response for three discrete bias states is presented

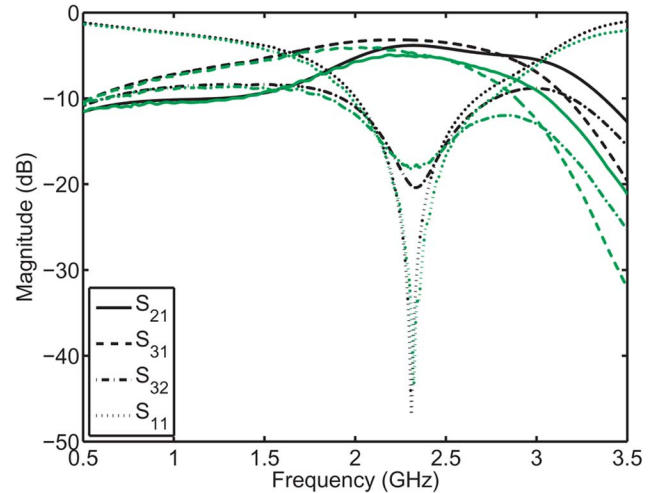


Fig. 11. Measured S -parameters at $U_{\text{bias}} = 15$ V (green in online version) and simulated data (black) for the tunable branch-line coupler prototype.

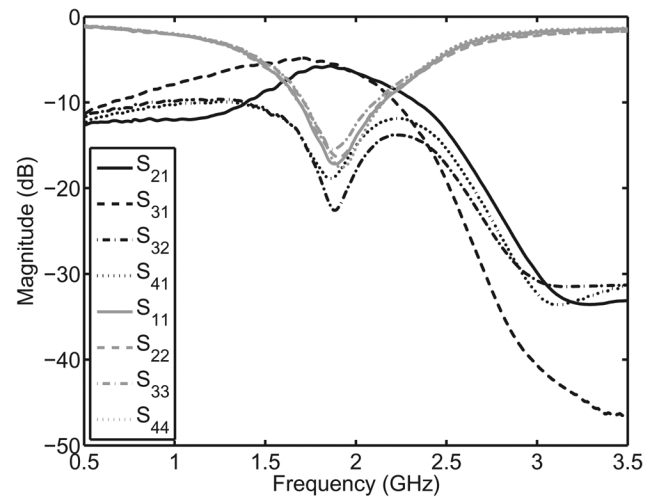


Fig. 12. Measured transmission and reflection S -parameters for tunable branch-line coupler prototype at bias state $U_{\text{bias}} = 5$ V.

in Figs. 12–14. All transmission and reflection parameters exhibit the well known branch-line coupler performance which achieves symmetric power splitting for two ports with simultaneous matching and isolation for all other ports. A continuous tuning region from 1.8 to 2.3 GHz is obtained. Similar to the implemented power divider the circuit indicates its low-pass characteristic, since higher order harmonics are suppressed in the transmission paths. Operating these couplers along with multi band power amplifiers, e.g., in a Doherty topology [30], would result in frequency agile transmitter stages with suppressed harmonic radiation and thus improved spectrum purity.

Additional to the ideal 3 dB coupling, the insertion loss varies from 2 to 2.7 dB depending on the applied bias state. The amplitude and phase difference between the two transmission paths is shown in Fig. 15. The worst case deviation from the nominal phase difference of 90° is $\pm 5^\circ$. Similar low differences are observed for the amplitude where the maximum difference for each bias state is 0.4 dB. Thus, the coupler operation is fulfilled at different operating frequencies.

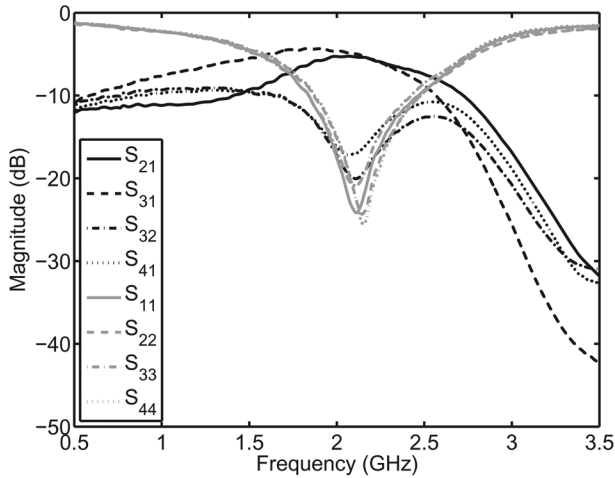


Fig. 13. Measured transmission and reflection S -parameters for tunable branch-line coupler prototype at bias state $U_{\text{bias}} = 9$ V.

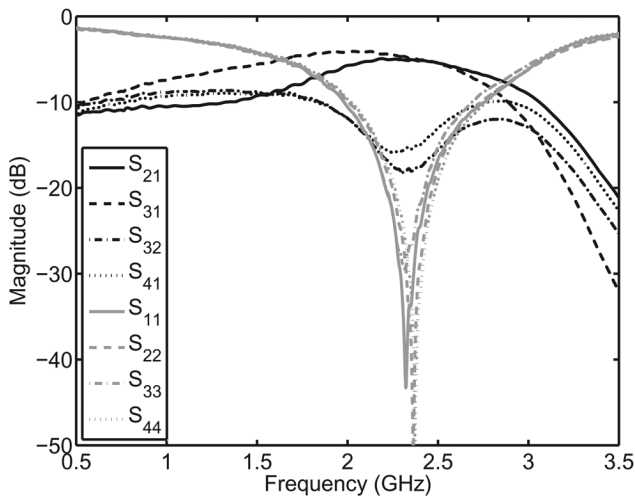


Fig. 14. Measured transmission and reflection S -parameters for tunable branch-line coupler prototype at bias state $U_{\text{bias}} = 15$ V.

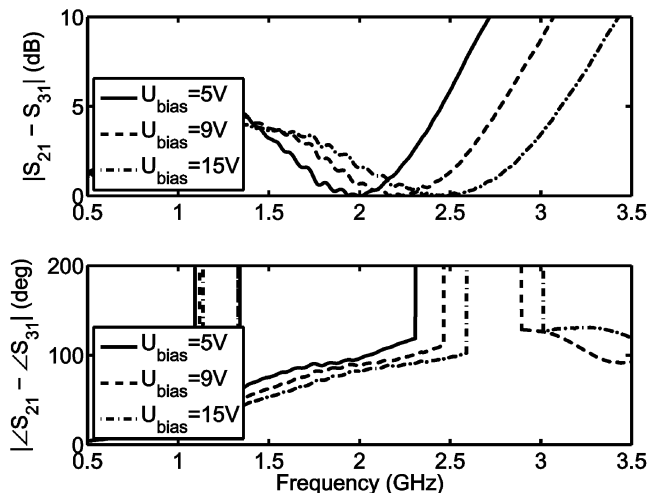


Fig. 15. Measured amplitude (top) and phase difference (bottom) for the transmission paths of the branch-line coupler.

VI. CONCLUSION

A novel design approach for tunable and reduced size microwave circuits is presented based on ferroelectric thin-film varactors. To our knowledge, this is the first successfully implemented tunable and reduced size power divider and branch-line coupler design based on a transmission line approach. The design methodology applies for quarter-wavelength based circuits and is fully scalable for different impedances and frequency regions. The operating principle is based on the substitution of the $\lambda/4$ transmission line segments with their equivalent low-pass structures. Ferroelectric varactors are used as tuning elements. Besides size reduction the novel functionality of tunability enabling frequency agile subsystems is achieved. The proposed methodology is verified by two prototype boards. The implemented Wilkinson power divider can be tuned continuously from 1.7 to 2.1 GHz. While the narrowband behavior of the original Wilkinson divider topology is retained, an improved isolation between the two output ports is achieved over a broad frequency region. The implemented branch-line coupler achieves a tuning region from 1.8 to 2.3 GHz while exhibiting symmetrical power coupling and the desired phase difference for the transmission paths. Additionally, the inherent low-pass characteristic for all transmission paths is beneficial in terms of higher order harmonics suppression. Further improvement of the varactor quality factors would result in implementations with performance improvement in terms of losses. Both frequency agile topologies are suitable for multi band operation in reconfigurable front-end systems.

REFERENCES

- [1] A. Tombak, F. Ayguavives, J.-P. Maria, G. Staaf, A. Kingon, and A. Mortazawi, "Tunable RF filters using thin film barium strontium titanate based capacitors," in *IEEE MTT-S Int. Microw. Symp. Dig.*, May 20–25, 2001, vol. 3, pp. 1453–1456.
- [2] J. Nath, D. Ghosh, J. Maria, A. Kingon, W. Fathelbab, P. Franzon, and M. Steer, "An electronically tunable microstrip bandpass filter using thin-film barium—strontium-titanate (BST) varactors," *IEEE Trans. Microw. Theory Tech.*, vol. 53, no. 9, pp. 2707–2712, Sep. 2005.
- [3] D. Kim, S.-S. Je, J. Kenney, and P. Marry, "Design of ferroelectric phase shifters for minimum performance variation over temperature," in *IEEE MTT-S Int. Microw. Symp. Dig.*, Jun. 6–11, 2004, vol. 1, pp. 257–260.
- [4] D. Kim, Y. Choi, M. Allen, J. Kenney, and D. Kiesling, "A wide-band reflection-type phase shifter at S -band using BST coated substrate," *IEEE Trans. Microw. Theory Tech.*, vol. 50, no. 12, pp. 2903–2909, Dec. 2002.
- [5] M. Schmidt, E. Lourandakis, A. Leidl, S. Seitz, and R. Weigel, "A comparison of tunable ferroelectric Π and T-matching networks," in *Proc. 37th Eur. Microw. Conf.*, Oct. 9–12, 2007, pp. 98–101.
- [6] P. Scheele, F. Goelden, A. Giere, S. Mueller, and R. Jakob, "Continuously tunable impedance matching network using ferroelectric varactors," in *IEEE MTT-S Int. Microw. Symp. Dig.*, Jun. 12–17, 2005, pp. 603–606.
- [7] Y. Liu, T. Taylor, J. Speck, and R. York, "High-isolation BST-MEMs switches," in *IEEE MTT-S Int. Microw. Symp. Dig.*, Jun. 2–7, 2002, vol. 1, pp. 227–230.
- [8] G. Subramanyam, F. Ahamed, and R. Biggers, "A Si MMIC compatible ferroelectric varactor shunt switch for microwave applications," *IEEE Microw. Wireless Compon. Lett.*, vol. 15, no. 11, pp. 739–741, Nov. 2005.
- [9] W. Fathelbab and M. Steer, "New classes of miniaturized planar marchand baluns," *IEEE Trans. Microw. Theory Tech.*, vol. 53, no. 4, pp. 1211–1220, Apr. 2005.

[10] A. Victor, J. Nath, D. Ghosh, B. Boyette, J.-P. Maria, M. Steer, A. Kingon, and G. Stauf, "A voltage controlled oscillator using barium strontium titanate (BST) thin film varactor," in *IEEE Radio Wireless Conf.*, Sep. 19–22, 2004, pp. 91–94.

[11] M. Al-Ahmad, C. Loyez, N. Rolland, and P. Rolland, "Wide BST-based tuning of voltage controlled oscillator," in *Asia-Pacific Microw. Conf.*, Dec. 12–15, 2006, pp. 468–471.

[12] H. Katta, H. Kurioka, and Y. Yashima, "Tunable power amplifier using thin-film BST capacitors," in *IEEE MTT-S Int. Microw. Symp. Dig.*, Jun. 11–16, 2006, pp. 564–567.

[13] A. Tombak, "A ferroelectric-capacitor-based tunable matching network for quad-band cellular power amplifiers," *IEEE Trans. Microw. Theory Tech.*, vol. 55, no. 2, pp. 370–375, Feb. 2007.

[14] E. Lourandakis, M. Schmidt, A. Leidl, S. Seitz, and R. Weigel, "A tunable and reduced size power divider using ferroelectric thin-film varactors," in *IEEE MTT-S Int. Microw. Symp. Dig.*, Jun. 15–20, 2008, pp. 967–970.

[15] E. Wilkinson, "An N -way hybrid power divider," *IEEE Trans. Microw. Theory Tech.*, vol. MTT-8, no. 1, pp. 116–118, Jan. 1960.

[16] E. A. Fardin, A. S. Holland, and K. Ghorbani, "Frequency agile 90° hybrid coupler using barium strontium titanate varactors," in *IEEE MTT-S Int. Microw. Symp. Dig.*, Jun. 3–8, 2007, pp. 675–678.

[17] G. Subramanyam, F. Miranda, R. Romanofsky, F. V. Keuls, C. Canedy, S. Aggarwal, T. Venkatesan, and R. Ramesh, "A ferroelectric tunable microstrip lange coupler for K -band applications," in *IEEE MTT-S Int. Microw. Symp. Dig.*, Jun. 11–16, 2000, vol. 3, pp. 1363–1366.

[18] M. Rahman, K. Shamsaifar, P. Inc, and M. Columbia, "Electronically tunable LTCC based multi-layer filter for mobile handset application," in *IEEE MTT-S Int. Microw. Symp. Dig.*, Jun. 8–13, 2003, vol. 3, pp. 1767–1770.

[19] M. Nguyen, W. Yan, and E. Horne, "Broadband tunable filters using high Q passive tunable ICs," in *IEEE MTT-S Int. Microw. Symp. Dig.*, Jun. 15–20, 2008, pp. 951–954.

[20] J. Nath, D. Ghosh, J. Maria, M. Steer, A. Kingon, and G. Stauf, "Microwave properties of BST thin film interdigital capacitors on low cost alumina substrates," in *Proc. 34th Eur. Microw. Conf.*, Oct. 11–15, 2004, pp. 1497–1500.

[21] Y. Cheng, N. Chong, Y. Wang, J. Liu, H. Chan, and C. Choy, "Microwave characterization of BST thin films on LAO interdigital capacitor," *Integr. Ferroelect.*, vol. 55, no. 1, pp. 939–946, 2003.

[22] J. Lu, S. Schmidt, D. Boesch, N. Pervez, R. York, and S. Stemmer, "Low-loss tunable capacitors fabricated directly on gold bottom electrodes," *Appl. Phys. Lett.*, vol. 88, pp. 112905–112905, 2006.

[23] P. Rundqvist, T. Liljenfors, A. Vorobiev, E. Olsson, and S. Gevorgian, "The effect of SiO₂, Pt, and Pt/Au templates on the microstructure and permittivity of BaSrTiO films," *J. Appl. Phys.*, vol. 100, pp. 114–116, 2006.

[24] D. Chase, L. Chen, and R. York, "Modeling the capacitive nonlinearity in thin-film BST varactors," *IEEE Trans. Microw. Theory Tech.*, vol. 53, no. 10, pp. 3215–3220, Oct. 2005.

[25] B. Strukov and A. Levanyuk, *Ferroelectric Phenomena in Crystals*. Berlin, Germany: Springer, 1998.

[26] S. Tappe, U. Bottger, and R. Waser, "Electrostrictive resonances in (Ba_{0.7}Sr_{0.3})TiO₃ thin films at microwave frequencies," *Appl. Phys. Lett.*, vol. 85, pp. 624–626, 2004.

[27] S. Gevorgian, A. Vorobiev, and J. Berge, "Electromechanical modeling and reduction of the electroacoustic losses in parallel-plate ferroelectric varactors," in *Proc. 36th Eur. Microw. Conf.*, Sep. 10–15, 2006, pp. 851–853.

[28] M. Schmidt, E. Lourandakis, R. Weigel, A. Leidl, and S. Seitz, "A thin-film BST varactor model for linear and nonlinear circuit simulations for mobile communication systems," in *2006 IEEE Int. Appl. Ferroelect. Symp.*, Aug. 30, 2006, pp. 372–375.

[29] T. Hirota, A. Minakawa, and M. Muraguchi, "Reduced-size branch-line and rat-race hybrids for uniplanar MMIC's," *IEEE Trans. Microw. Theory Tech.*, vol. 38, no. 3, pp. 270–275, Mar. 1990.

[30] W. Doherty, "A new high efficiency power amplifier for modulated waves," *Proc. IRE*, vol. 24, no. 9, pp. 1163–1182, Sep. 1936.



Errikos Lourandakis (S'06–M'06) was born in Nuremberg, Germany, in 1981. He received the Dipl. Eng. degree in electrical engineering from the University of Patras, Patras, Greece, in 2005, and is currently working toward his Ph.D. degree at the University of Erlangen–Nuremberg, Erlangen, Germany.

tunable microwave circuits.

In 2005, he joined the Institute for Electronics Engineering, University of Erlangen–Nuremberg. His research interests concern the field of microwave engineering with a focus on frequency agile and

Matthias Schmidt (S'04–M'07) was born in Neuendettelsau, Germany, in 1977. He received the Dipl.-Ing. and Dr.-Ing. degrees in electrical engineering from the Friedrich-Alexander University Erlangen–Nuremberg, Erlangen, Germany, in 2003 and 2007, respectively.

From 2003 to 2007, he was with the Institute for Electronics Engineering, University of Erlangen–Nuremberg, as a Research Assistant. He was engaged in the development and investigation of tunable microwave circuits based on ferroelectric capacitors. In 2007, he joined the Research and Development New Products Department EPCOS AG, Munich, Germany, where he has been involved in development of RF and microwave components.

Stefan Seitz (M'07) was born in Dillingen, Germany, in 1956. He received the Dipl.-Ing. and Dr.-Ing. degrees in electrical engineering from the Munich University of Technology, Munich, Germany.

From 1984 to 1990, he was a Research Engineer, and from 1990 to 1999, a Department Manager with the Fraunhofer Institute of Solid State Technology, Munich, Germany. In 1999, he joined EPCOS AG, Munich, Germany. Since 2003, he has been Vice President of the Research and Development New Products Department, where he is responsible for innovative products. He has been engaged in research and development on microcontroller systems, mixed-signal ASIC design, semiconductor and MEMS technology, high-temperature electronics, and RF front-end modules.



Robert Weigel (S'88–M'89–SM'95–F'02) was born in Ebermannstadt, Germany, in 1956. He received the Dr.-Ing. and Dr.-Ing.habil. degrees in electrical engineering and computer science from the Munich University of Technology, Munich, Germany, in 1989 and 1992, respectively.

From 1982 to 1988, he was a Research Engineer, from 1988 to 1994, a Senior Research Engineer, and from 1994 to 1996, a Professor of RF circuits and systems with the Munich University of Technology. In winter 1994/1995, he was a Guest Professor of SAW technology with the Vienna University of Technology, Vienna, Austria. From 1996 to 2002, he was Director of the Institute for Communications and Information Engineering, University of Linz, Linz, Austria. In August 1999, he cofounded Danube Integrated Circuit Engineering (DICE), Linz, Germany, an Infineon Technologies Design Center, which is devoted to the design of mobile radio circuits and systems. In 2000, he became a Professor of RF engineering with Tongji University, Shanghai, China. In 2000, he also cofounded the Linz Center of Competence in Mechatronics. Since 2002, he has been Head of the Institute for Electronics Engineering, University of Erlangen–Nuremberg, Erlangen, Germany. He is editor of the *Proceedings of the European Microwave Association* (EuMA).

Dr. Weigel is a member of the Institute for Components and Systems of The Electromagnetics Academy. He is a member of the German ITG and the Austrian ÖVE. Within the IEEE Microwave Theory and Techniques Society (IEEE MTT-S), he has been chair of the Austrian COM/MTT Joint Chapter, Region 8 coordinator. From 2001 to 2003, he was an IEEE MTT-S Distinguished Microwave Lecturer. He is an Administrative Committee (AdCom) member and vice-chair of MTT-2 Microwave Acoustics.